

# A RELM earthquake forecast based on pattern informatics

James R. Holliday<sup>1,2</sup>, Chien-chih Chen<sup>3,2</sup>, Kristy F. Tiampo<sup>4</sup>,  
John B. Rundle<sup>2,1</sup>, Donald L. Turcotte<sup>5</sup>, and Andrea Donnellan<sup>6</sup>

<sup>1</sup> Department of Physics - University of California, Davis, USA

<sup>2</sup> Computational Science and Engineering Center - University of California, Davis, USA

<sup>3</sup> National Central University - Taiwan

<sup>4</sup> Department of Earth Sciences - University of Western Ontario, Canada

<sup>5</sup> Geology Department - University of California, Davis, USA

<sup>6</sup> NASA Jet Propulsion Laboratory, USA

## Abstract

We present a RELM forecast of future earthquakes in California that is primarily based on the pattern informatics (PI) method. This method identifies regions that have systematic fluctuations in seismicity, and it has been demonstrated to be successful. A PI forecast map originally published on 19 February 2002 for southern California successfully forecast the locations of sixteen of eighteen  $M > 5$  earthquakes during the past three years. The method has also been successfully applied to Japan and on a worldwide basis. An alternative approach to earthquake forecasting is the relative intensity (RI) method. The RI forecast map is based on recent levels of seismic activity of small earthquakes. Recent advances in the PI method show considerable improvement, particularly when compared with the RI method using relative operating characteristic (ROC) diagrams for binary forecasts. The RELM application requires a probability for each location for a number of magnitude bins over a five year period. We have therefore constructed a hybrid forecast in which we combine the PI method with the RI method to compute a map of probabilities for events occurring at any location, rather than just the most probable locations. These probabilities are further converted, using Gutenberg-Richter scaling laws, to anticipated rates of future earthquakes that can be evaluated using the RELM test.

## 1 Introduction

There have been a wide variety of approaches applied to the forecasting of earthquakes (Turcotte, 1991; Kanamori, 2003). These approaches can be divided into two general classes; the first is based on empirical observations of precursory changes. Examples include precursory seismic activity, precursory ground motions, and many others. The second approach is based on statistical patterns of seismicity. Neither approach has been able to provide reliable short-term forecasts (days to months) on a consistent basis.

Although short-term predictions are not available, long-term seismic-hazard assessments can be made. A large fraction of all earthquakes occur in the vicinity of plate boundaries, although some do occur in plate interiors. It is also possible to assess the long-term probability of having an earthquake of a specified magnitude in a specified region. These assessments are primarily based on the hypothesis that future earthquakes will occur in regions where past, typically large, earthquakes have occurred (Kossobokov et al., 2000). As we will discuss, a more promising approach is to begin with the hypothesis that the rate of occurrence of small earthquakes in a region can be analyzed to assess the probability of occurrence of much larger earthquakes.

The RELM forecast described in this paper is primarily based on the pattern informatics (PI) method (Rundle et al., 2002; Tiampo et al., 2002c,a; Rundle et al., 2003). This method identifies regions of strongly correlated fluctuations in seismic activity. These regions are the locations where subsequent large earthquakes have been shown to occur,

therefore indicating a strong association with the high stress preceding the main shock. The fluctuations in seismicity rate revealed in a PI map have been found to be related to the preparation process for large earthquakes. Seismic quiescence and seismic activation (Bowman et al., 1998; Wyss and Habermann, 1988), which are revealed by the PI map, are examples of such preparation processes. The PI method identifies the existence of correlated regions of seismicity in observational data that precede the main shock by months and years. The fact that this correlated region locates the aftershocks as well as main shocks leads us to identify this region of correlated seismicity with the region of correlated high stress (Tiampo et al., 2002b,c,a). Finally, our results with the PI map indicate that the occurrences of future significant earthquakes are better forecasted by a change (correlated fluctuation) in the average seismicity rate rather than with the high seismicity rate itself.

The PI method does not predict earthquakes, rather it forecasts the regions (hotspots) where earthquakes are most likely to occur in the relatively near future (typically five to ten years). The objective is to reduce the areas of earthquake risk relative to those given by long-term hazard assessments. The result is a map of areas in a seismogenic region (hotspots) where earthquakes are likely to occur during a specified period in the future. In this paper a PI map is combined with historic seismicity data to produce a map of probabilities for future large events. These probabilities can be further converted, using Gutenberg-Richter scaling laws, to forecast rates of occurrence of future earthquakes in specific magnitude ranges. This forecast can be evaluated using the RELM model. In the following we present details of the PI method and the procedure for producing a composite forecast map. A discussion on binary forecasts and forecast verification techniques is given in the appendix.

## 2 The PI method

Our approach divides the seismogenic region to be studied into a grid of square boxes, or “pixels”, whose size is related to the magnitude of the earthquakes to be forecast. The rates of seismicity in each box are studied to quantify anomalous behavior. The basic idea is that any seismicity precursors represent changes, either a local increase or decrease of seismic activity, so our method identifies the locations in which these changes are most significant during a predefined change interval. The subsequent forecast interval is the five year time window during which the forecast is valid. The box size is selected to be consistent with the correlation length associated with accelerated seismic activity (Bowman et al., 1998), and the minimum earthquake magnitude considered is the lower limit of sensitivity and completeness of the network in the region under consideration. The PI method as applied to California in this paper is composed of the following steps:

1. The seismically active region is binned into boxes of size  $0.1^\circ \times 0.1^\circ$  and all events having  $M \geq 3.0$  are used. These boxes are labeled  $x_i$ . This is also the box size specified for the RELM forecast.

2. The seismicity obtained from the ANSS catalog for each day in each box is uniformly spread over that box and the eight immediately adjacent boxes (the Moore neighborhood (Moore, 1962)). The resulting smoothed intensities for each box is a time series.
3. Only the top 10% most active boxes are considered. These are the boxes with the most  $M_c \geq 3.0$  earthquakes during the period  $t_0 = 1$  January 1950 to  $t_2 = 1$  August 2005.  $M_c$  is the cutoff magnitude for the analysis.
4. Each time series is normalized in time by subtracting the temporal mean and dividing by the temporal standard deviation.
5. Each time series is then normalized in space for each value of time by subtracting the spatial mean and dividing by the spatial standard deviation.
6. Two intensity maps  $I_1(x_i, t_b, t_1)$ ,  $I_2(x_i, t_b, t_2)$  are computed by averaging all the time series from an initial time,  $t_b$  to  $t_1$  where  $t_0 < t_b < t_1$ , and then from  $t_b$  to  $t_2$ . Here  $t_0 = 1$  January 1950,  $t_1 = 1$  January 1985, and  $t_2 = 1$  August 2005.
7. The intensity change  $\Delta I(x_i, t_b, t_1, t_2) = I_2(x_i, t_b, t_2) - I_1(x_i, t_b, t_1)$  is computed at each location and absolute value is taken  $|\Delta I(x_i, t_b, t_1, t_2)|$ .
8. The average of  $|\Delta I(x_i, t_b, t_1, t_2)|$  over all values of  $t_0 < t_b < t_{max}$  is then computed.
9. Finally, the mean squared change  $< |\Delta I(x_i, t_b, t_1, t_2)|^2 >$  is computed.

Note that steps (2), (3), (7), and (8) have been modified from the original, published algorithm (Rundle et al., 2002; Tiampo et al., 2002c,a; Rundle et al., 2003).

Hotspot pixels are defined to be the regions where  $\Delta P_i(t_0, t_1, t_2)$  is larger than some threshold value in the interval  $[0, 1]$ . In these regions,  $P_i(t_0, t_1, t_2)$  is larger than the average value for all boxes (the background level). Note that since the intensities are squared in defining probabilities the hotspots may be due to either increases of seismic activity during the change time interval (activation) or due to decreases (quiescence). We hypothesize that earthquakes with magnitudes larger than  $M_c + 2$  will occur preferentially in hotspots during the forecast time interval  $t_2$  to  $t_3$ . Note that this is a binary forecast: either an earthquake is forecast to occur or it is forecast not to occur.

### 3 Relative intensity

An alternative approach to earthquake forecasting is to use the rate of occurrence of small earthquakes in the past. We refer to this type of forecast as a relative intensity (RI) forecast. In such a forecast, the study region is again tiled with boxes of size  $0.1^\circ \times 0.1^\circ$ . The number of earthquakes with magnitude  $M \geq 3.0$  in each box is determined over the time period from  $t_0$  to  $t_2$ . The RI score for each box is then computed as the total number of earthquakes in the box in the time period divided by the value for the box having the largest value. In order to create a binary forecast, a threshold value in the interval  $[0, 1]$  is selected. Large earthquakes having  $M \geq 5$  are then considered possible only in boxes having an RI value larger than the threshold. The physical justification for this type of forecast is that large earthquakes are considered most likely to occur at sites of high seismic activity. In this paper we combine our binary PI forecast with a continuum RI forecast in order to create our continuum RELM forecast.

## 4 Binary versus continuum forecasts

The earthquake forecast made by the PI method is a binary forecast. An earthquake is forecast to occur in the hotspot regions and not to occur in the other regions, analogous to the issuance of tornado warnings. An extensive methodology has been developed in the atmospheric sciences for forecast verification. A standard approach uses contingency tables and relative operating characteristic (ROC) diagrams (Jolliffe and Stephenson, 2003). An example of binary forecast construction and verification is presented in the appendix.

The alternative to binary forecasts is a continuum forecast. The likelihood of an earthquake throughout the entire region is specified, analogous to temperature forecasts in the atmospheric sciences. A common approach to testing the validity of these forecasts is the maximum likelihood test. Kagan and Jackson (2000) were the first to apply this test to earthquake forecasts. The maximum likelihood test is not appropriate for the verification of binary forecasts because they are overly sensitive to the least probable events. For example, consider two forecasts. The first perfectly forecasts 99 out of 100 events but assigns zero probability to the last event. The second assigns zero probability to all 100 events. Under a likelihood test, both forecasts will have the same skill score of  $-\infty$ . Furthermore, a naive forecast that assigns uniform probability to all possible sites will always score higher than a forecast that misses only a single event but is otherwise superior.

## 5 Creating the forecast map

The PI method finds regions where earthquakes are most likely to occur during a future time window. In order to create a forecast map suitable for RELM testing, we combined the PI map with the RI map to create a probability map. This map is then renormalized to unit probability and scaled by the total number of  $M \geq 5$  earthquakes expected over the future five year period. The details of this procedure are as follows:

1. We first create a relative intensity map for the entire region to be considered. Data was taken from the ANSS on-line catalog for the years 1950 to 2005. This data was then truncated such that relative values greater than  $10^{-1}$  were set to  $10^{-1}$  and non-zero values less than  $10^{-4}$  were set to  $10^{-4}$ . Finally, since the RELM calculations cannot handle zero-rate values, every box with zero historic seismicity was given a value of  $10^{-5}$ . The RI map is shown in Figure 1A.
2. We next perform a pattern informatics calculation over the top 10% of most active sites in California using the ANSS catalog as input. For this calculation, we used  $t_0 = 1$  January 1950,  $t_1 = 1$  January 1985, and  $t_2 = 1$  August 2005. Since the hotspots are where we expect future earthquakes to occur, they are given a probability value of unity. The PI map is shown in Figure 1B.
3. We then create a composite probability map by superimposing the PI map and its Moore neighborhood (the pixel plus its eight adjacent neighbors) on top of the RI map. All the hotspot pixels have a probability of 1, and all other pixels have probabilities that range from  $10^{-5}$  to  $10^{-1}$ . The composite map is shown in Figure 2.
4. To convert our pixel probabilities to earthquake occurrence probabilities, we first add up the probabilities in all pixels in the region and call this sum  $N$ . We then normalize this total to the expected number of  $M \geq 5.0$  earthquakes during the forecast period. We estimate four to eight such events per year and assume 30 such events during a five year period. In order to do this, we multiply each pixel probability by  $30/N$  to give our RELM forecast. We then use Gutenberg-Richter scaling to interpolate these rates into the appropriate magnitude bins specified by the RELM test.

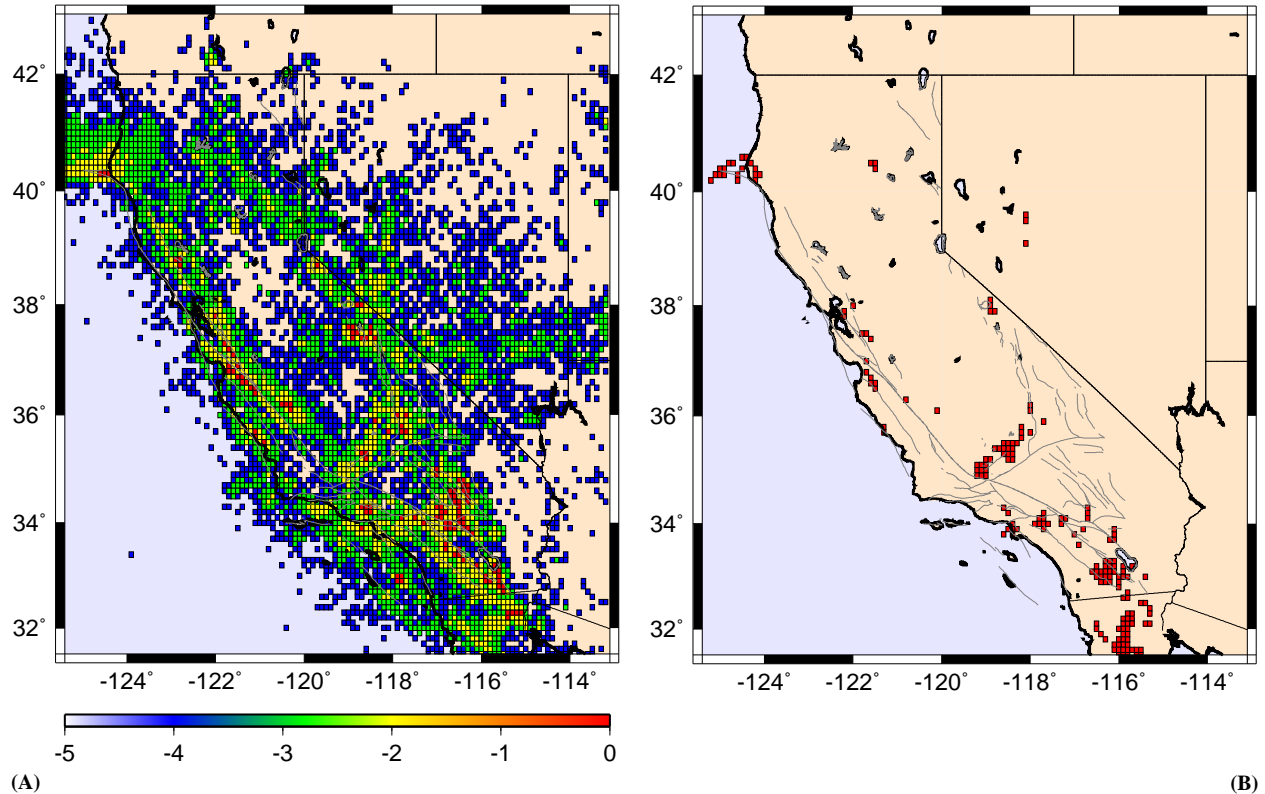


Figure 1: (A) Relative intensity (RI) map for all of California and the surrounding region. Data from the ANSS on-line catalog for the years 1950 to 2005 were used. (B) Pattern informatics (PI) map for the same region and time frame as above.

## 6 Discussion

Ultimately there exists the fundamental question of whether forecasts of the time and location of future earthquakes can be accurately made. It is accepted that long term hazard maps of the expected rate of occurrence of earthquakes are reasonably accurate. But is it possible to do better? Are there precursory phenomena that will allow earthquakes to be forecast?

It is actually quite surprising that immediate local precursory phenomena are not seen. Prior to a volcanic eruption, increases in regional seismicity and surface movements are generally observed. For a fault system, the stress gradually increases until it reaches the frictional strength of the fault and a rupture is initiated. It is certainly reasonable to hypothesize that the stress increase would cause increases in background seismicity and aseismic slip. In order to test this hypothesis the Parkfield Earthquake Prediction Experiment was initiated in 1985. The expected Parkfield earthquake occurred beneath the heavily instrumented region on 28 September 2004. No local precursory changes were observed (Lindh, 2005).

In the absence of local precursory signals, the next question is whether broader anomalies develop, and in particular whether there is anomalous seismic activity. It is this question that is addressed in this paper. Using a technique that has been successfully applied to the forecasting of El Niño we have developed a systematic pattern informatics (PI) approach to the identification of regions of anomalous seismic activity. Applications of this technique to California, Japan, and on a world-wide basis have successfully forecast the location of future earthquakes. We emphasize that this is not an earthquake prediction. It is a forecast of where future earthquakes are expected to occur during a future time window of

five to ten years. The objective is to reduce the possible future sites of earthquakes relative to a long term hazard assessment map.

## Acknowledgments

This work has been supported by NASA Headquarters under the Earth System Science Fellowship Grant NGT5 (JRH), by research support from the National Science Council and the Department of Earth Sciences (CCC), by an HSERC Discovery grant (KFT), by a grant from the US Department of Energy, Office of Basic Energy Sciences to the University of California, Davis DE-FG03-95ER14499 (JRH and JBR), and through additional funding from NSF grant ATM-0327558 (DLT) and the National Aeronautics and Space Administration under grants through the Jet Propulsion Laboratory (AD) to the University of California, Davis.

## Appendix A - Forecast verification

Along with the RELM model, previous published tests of earthquake forecasts have emphasized the likelihood test (Kagan and Jackson, 2000; Rundle et al., 2002; Tiampo et al., 2002c; Holliday et al., 2005). As discussed above, these tests have the significant disadvantage that they are overly sensitive to the least probable events. For this reason, likelihood tests are subject to unconscious bias.

An extensive review on forecast verification in the atmospheric sciences has been given by Jolliffe and Stephenson (2003). The wide variety of approaches that they consider are directly applicable to earthquake forecasts as well. We believe that many of these approaches are better suited to the evaluation of earthquake forecasts. The earthquake

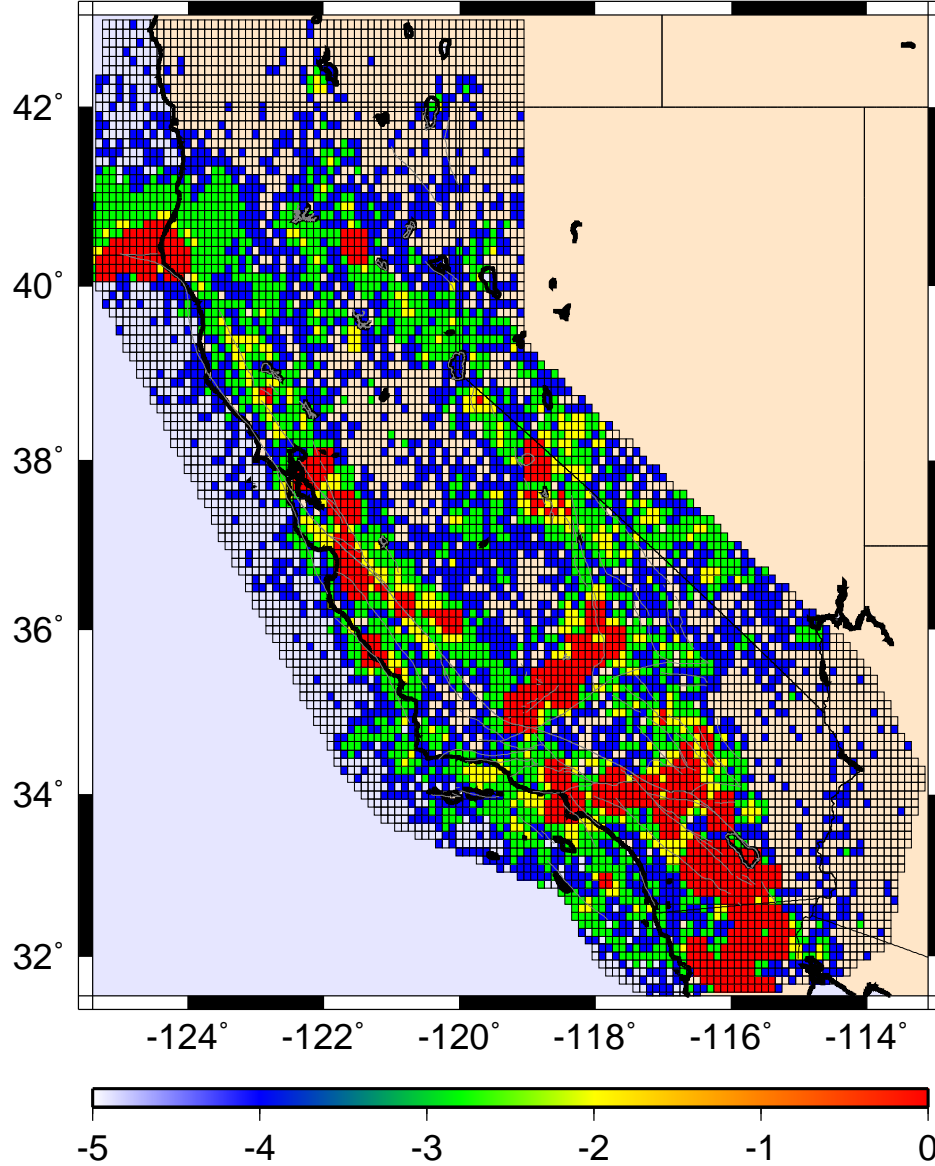


Figure 2: Composite forecast map. The scaled PI and RI maps have been combined, and boxes outside the testing region have been discarded.

forecasts considered in this paper can be viewed as binary forecasts by considering the events (earthquakes) as being forecast either to occur or not to occur in a given box. We consider that there are four possible outcomes for each box, thus two ways to classify each hotspot, box, and two ways to classify each non-hotspot, box:

1. An event occurs in a hotspot box or within the Moore neighborhood of the box (the Moore neighborhood is comprised of the eight boxes surrounding the forecast box). This is a success.
2. No event occurs in a white non-hotspot box. This is also a success.
3. No event occurs in a hotspot box or within the Moore neighborhood of the hotspot box. This is a false alarm.
4. An event occurs in a white, non-hotspot box. This is a failure to forecast.

We note that these rules tend to give credit, as successful forecasts, for events that occur very near hotspot boxes. We have adopted these rules in part because the grid of boxes is positioned arbitrarily on the seismically active region, thus we allow a margin of error of  $\pm 1$  box dimension. In addition, the events we are forecasting are large enough so that their source dimension approaches, and can even exceed, the box dimension meaning that an event might have its epicenter outside a hotspot box, but the rupture might then propagate into the box. Other similar rules are possible but we have found that all such rules basically lead to similar results.

The standard approach to the evaluation of a binary forecast is the use of a relative operating characteristic (ROC) diagram (Swets, 1973; Mason, 2003). Standard ROC diagrams consider the fraction of failures-to-predict and the fraction of false alarms. This method evaluates the performance of the forecast method relative to random chance by con-

structing a plot of the fraction of failures to predict against the fraction of false alarms for an ensemble of forecasts. Molchan (Molchan, 1997) has used a modification of this method to evaluate the success of intermediate term earthquake forecasts.

The binary approach has a long history, over 100 years, in the verification of tornado forecasts (Mason, 2003). These forecasts take the form of a tornado forecast for a specific location and time interval, each forecast having a binary set of possible outcomes. For example, during a given time window of several hours duration, a forecast is issued in which a list of counties is given with a statement that one or more tornadoes will or will not occur. A  $2 \times 2$  contingency table is then constructed, the top row contains the counties in which tornadoes are forecast to occur and the bottom row contains counties in which tornadoes are forecast to not occur. Similarly, the left column represents counties in which tornadoes were actually observed, and the right column represents counties in which no tornadoes were observed.

With respect to earthquakes, our forecasts take exactly this form. A time window is proposed during which the forecast of large earthquakes having a magnitude above some minimum threshold is considered valid. An example might be a forecast of earthquakes larger than  $M = 5$  during a period of five or ten years duration. A map of the seismically active region is then completely covered ("tiled") with boxes of two types: boxes in which the epicenters of at least one large earthquake are forecast to occur and boxes in which large earthquakes are forecast to not occur. In other types of forecasts, large earthquakes are given some continuous probability of occurrence from 0% to 100% in each box (Kagan and Jackson, 2000). These forecasts can be converted to the binary type by the application of a *threshold* value. Boxes having a probability below the threshold are assigned a forecast rating of *non-occurrence* during the time window, while boxes having a probability above the threshold are assigned a forecast rating of *occurrence*. A high threshold value may lead to many *failures to predict* (events that occur where no event is forecast), but few *false alarms* (an event is forecast at a location but no event occurs). The level at which the threshold is set is then a matter of public policy specified by emergency planners, representing a balance between the prevalence of failures to predict and false alarms.

## Appendix B - Binary earthquake forecast verification

To illustrate this approach to earthquake forecast verification, we have constructed two types of retrospective binary forecasts for California. The first type of forecast utilizes the PI results published by Rundle *et al.* and Tiampo *et al.* (Rundle *et al.*, 2002; Tiampo *et al.*, 2002c) for southern California and adjacent regions ( $32^\circ$  to  $38.3^\circ$  N lat,  $238^\circ$  to  $245^\circ$  E long). This forecast was constructed for the time period 1 January 2000 to 31 December 2009, but we performed an interim analysis using data up to the present. The second type of forecast utilizes the RI results with the same parameter thresholds.

The first step in our generation of ROC diagrams is the construction of the  $2 \times 2$  contingency table for the PI and RI forecast maps. The hotspot boxes in each map represent the forecast locations. A hotspot box upon which *at least* one large future earthquake during the forecast period occurs is counted as a *successful forecast*. A hotspot box upon which *no* large future earthquake occurs during the forecast period is counted as an *unsuccessful forecast*, or alternately, a *false alarm*. A white box upon which *at least* one large future earthquake during the forecast period occurs is counted as a *failure to forecast*. A white box upon which *no* large future earthquake occurs during the forecast period is counted as a *unsuccessful forecast of non-occurrence*.

Verification of the PI and RI forecasts proceeds in exactly the same way as for tornado forecasts. For a given number of hotspot boxes, which is controlled by the value of the probability threshold in each map, the

Table 1: Contingency tables as a function of false alarm rate. In Table 1A, a threshold value was chosen such that  $F \approx 0.005$ . In Table 1B, a threshold value was chosen such that  $F \approx 0.021$ .

(A)

Pattern informatics (PI) forecast			
Forecast	Observed		
	Yes	No	Total
Yes	(a) 4	(b) 25	29
No	(c) 13	(d) 4998	5011
Total	17	5023	5040

Relative intensity (RI) forecast			
Forecast	Observed		
	Yes	No	Total
Yes	(a) 2	(b) 27	29
No	(c) 14	(d) 4997	5011
Total	16	5024	5040

(B)

Pattern informatics (PI) forecast			
Forecast	Observed		
	Yes	No	Total
Yes	(a) 23	(b) 104	127
No	(c) 9	(d) 4904	4913
Total	32	5008	5040

Relative intensity (RI) forecast			
Forecast	Observed		
	Yes	No	Total
Yes	(a) 20	(b) 107	127
No	(c) 10	(d) 4903	4913
Total	30	5010	5040

contingency table (see Table 1) is constructed for both the PI and RI maps. Values for the table elements  $a$  (Forecast=yes, Observed=yes),  $b$  (Forecast=yes, Observed=no),  $c$  (Forecast=no, Observed=yes), and  $d$  (Forecast=no, Observed=no) are obtained for each map. The fraction of colored boxes, also called the *probability of forecast of occurrence*, is  $r = (a + b)/N$ , where the total number of boxes is  $N = a + b + c + d$ . The *hit rate* is  $H = a/(a + c)$  and is the fraction of large earthquakes that occur on a hotspot. The *false alarm rate* is  $F = b/(b + d)$  and is the fraction of non-observed earthquakes that are incorrectly forecast.

To analyze the information in the PI and RI maps, the standard procedure is to consider all possible forecasts together. These are obtained by increasing  $F$  from 0 (corresponding to no hotspots on the map) to 1 (all active boxes on the map are identified as hotspots). The plot of  $H$  versus  $F$  is the relative operating characteristic (ROC) diagram. Varying the threshold value for both the PI and RI forecasts, we have obtained the values of  $H$  and  $F$  given in Figure 3. The results corresponding to the contingency tables given in Table 1 are given by the filled symbols. The forecast with 29 hotspot boxes has  $F_{PI} = 0.00498$ ,  $H_{PI} = 0.235$  and  $F_{RI} = 0.00537$ ,  $H_{RI} = 0.125$ . The forecast with 127 hotspot boxes has  $F_{PI} = 0.0207$ ,  $H_{PI} = 0.719$  and  $F_{RI} = 0.0213$ ,  $H_{RI} = 0.666$ . Also shown in Figure 3 is a gain curve defined by the ratio of  $H_{PI}(F)$  to  $H_{RI}(F)$ . Gain values greater than unity indicate better performance using the PI map than using the RI map. The horizontal dashed line corresponds to zero gain. From Figure 3 it can be seen that the PI approach outperforms (is above) the RI under many circumstances and both outperform a random map, where  $H = F$ , by a large margin. For reference, ROC diagrams using the modified method discussed in the main text for the same forecast period

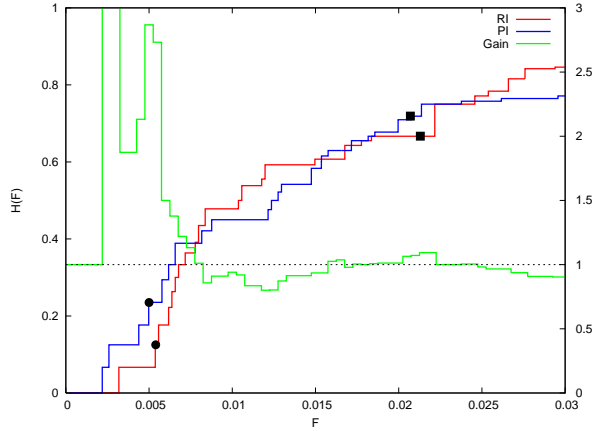


Figure 3: Relative operating characteristic (ROC) diagram. Plot of hit rates,  $H$ , versus false alarm rates,  $F$ , for the PI forecast and RI forecast. Also shown is the gain ratio defined as  $H_{PI}(F)/H_{RI}(F)$ . The filled symbols correspond to the threshold values used in Table 1, solid circles for 29 hotspot boxes and solid squares for 127 hotspot boxes. The horizontal dashed line corresponds to zero gain.

are given in Figure 4. Note that a different input catalog was used for this analysis. Also note that in this case, the PI approach outperforms the RI under all circumstances.

## References

- Bowman, D. D., Ouillon, G., Sammis, C. G., Sornette, A., and Sornette, D. (1998). An observational test of the critical earthquake concept. *J. Geophys. Res.*, 103:24359–24372.
- Holliday, J. R., Rundle, J. B., Tiampo, K. F., Klein, W., and Donnellan, A. (2005). Modification of the pattern informatics method for forecasting large earthquake events using complex eigenvectors. *Tectonophysics*, in press.
- Jolliffe, I. T. and Stephenson, D. B. (2003). *Forecast Verification*. John Wiley, Chichester.
- Kagan, Y. Y. and Jackson, D. D. (2000). Probabilistic forecasting of earthquakes. *Geophys. J. Int.*, 143:438–453.
- Kanamori, H. (2003). Earthquake prediction: An overview. In Lee, W. H. K., Kanamori, H., Jennings, P. C., and Kisslinger, C., editors, *International Handbook of Earthquake & Engineering Seismology*, pages 1205–1216, Amsterdam. Academic Press.
- Kossobokov, V. G., Keilis-Borok, V. I., Turcotte, D. L., and Malamud, B. D. (2000). Implications of a statistical physics approach for earthquake hazard assessment and forecasting. *Pure Appl. Geophys.*, 157:2323–2349.
- Lindh, A. G. (2005). Success and failure at Parkfield. *Seis. Res. Lett.*, 76:3–6.
- Mason, I. B. (2003). Binary events. In Jolliffe, I. T. and Stephenson, D. B., editors, *Forecast Verification*, pages 37–76, Chichester. John Wiley.
- Molchan, G. M. (1997). Earthquake predictions as a decision-making problem. *Pure Appl. Geophys.*, 149:233–247.

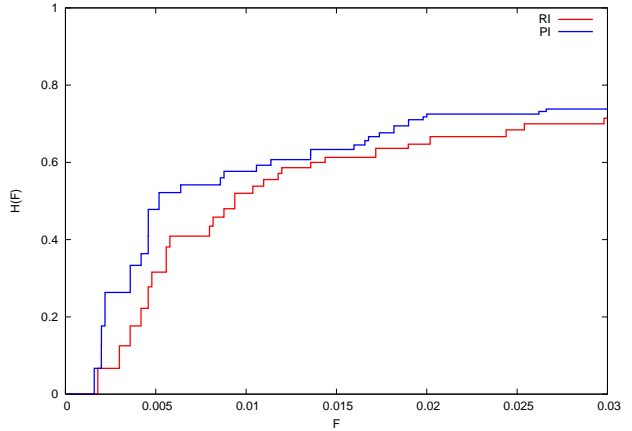


Figure 4: Relative operating characteristic (ROC) diagram. Plot of hit rates,  $H$ , versus false alarm rates,  $F$ , for the RI forecast and PI forecast using the modified method. Note that the PI approach outperforms the RI under all circumstances.

- Moore, E. F. (1962). Machine models of self reproduction. In *Proceedings of the Fourteenth Symposium on Applied Mathematics*, pages 17–33. American Mathematical Society.
- Rundle, J. B., Tiampo, K. F., Klein, W., and Martins, J. S. S. (2002). Self-organization in leaky threshold systems: The influence of near-mean field dynamics and its implications for earthquakes, neurobiology, and forecasting. *Proc. Natl. Acad. Sci. U. S. A.*, 99:2514–2521: Suppl. 1.
- Rundle, J. B., Turcotte, D. L., Shcherbakov, R., Klein, W., and Sammis, C. (2003). Statistical physics approach to understanding the multiscale dynamics of earthquake fault systems. *Rev. Geophys.*, 41(4):1019.
- Swets, J. A. (1973). The relative operating characteristic in psychology. *Science*, 182:990–1000.
- Tiampo, K. F., Rundle, J. B., McGinnis, S., Gross, S. J., and Klein, W. (2002a). Eigenpatterns in southern California seismicity. *J. Geophys. Res.*, 107(B12):2354.
- Tiampo, K. F., Rundle, J. B., McGinnis, S., Gross, S. J., and Klein, W. (2002b). Mean field threshold systems and earthquakes: An application to earthquake fault systems. *Europhys. Lett.*, 60(3):481–487.
- Tiampo, K. F., Rundle, J. B., McGinnis, S., and Klein, W. (2002c). Pattern dynamics and forecast methods in seismically active regions. *Pure Appl. Geophys.*, 159:2429–2467.
- Turcotte, D. L. (1991). Earthquake prediction. *An. Rev. Earth Planet. Sci.*, 19:263–281.
- Wyss, M. and Habermann, R. E. (1988). Precursory seismic quiescence. *Pure Appl. Geophys.*, 126:319–332.